Flow between a stationary and a rotating disk shrouded by a co-rotating cylinder

J. M. Lopez
Department of Mathematics and Earth Systems Science Center, The Pennsylvania State University, University Park, Pennsylvania 16802

(Received 26 April 1996; accepted 17 June 1996)

Boundary layers on stationary and rotating disks have received much attention since von Kármán's [Z. Angew. Math. Mech. **1**, 233 (1921)] and Bödewadt's [Z. Angew. Math. Mech. **20**, 241 (1940)] studies of the cases with disks of infinite radius. Theoretical treatments have focused on similarity treatments leading to conflicting ideas about existence and uniqueness, and where self-similar solutions exist, whether they are physically realizable. The coupling between the boundary layer flows and the interior flow between them, while being of practical importance in a variety of situations such as turbomachinery and ocean circulations, is not well understood. Here, a numerical treatment of the axisymmetric Navier–Stokes equations, together with some experiments for the case of finite stationary and rotating disks bounded by a co-rotating sidewall is presented. We show that in the long time limit, solutions are steady and essentially self-similar. Yet the transients are not. In particular, axisymmetric waves propagate in the stationary disk boundary layer when the vortex lines entering the boundary layer develop inflection points, and there are subsequent eruptions of vortical flow out of the boundary layer deep into the interior at large Reynolds numbers. © *1996 American Institute of Physics.* [S1070-6631(96)01410-9]

I. INTRODUCTION

The problem of laminar flow between two parallel disks has attracted much attention over the years. This attention stems from both practical, e.g., ocean circulation models and turbomachinery applications, and theoretical interests, e.g., exact solutions of the Navier–Stokes equations in certain geometric limiting cases. The literature is very extensive, and that referred to here is by no means exhaustive. Rott and Lewellen[1] review some of the outstanding issues at that time.

Theoretical work on this class of flows has been performed mainly in the framework of similarity solutions. As noted by Durlofsky and Brady,[2] the assumption of self-similarity to reduce the Navier–Stokes equations from partial differential equations to ordinary differential equations greatly simplifies the analysis, but there is no assurance as to whether the solutions are physically realizable. Within the self-similar framework, flow domains are often unbounded and the solutions possess singularities at infinity or the origin. While it is generally accepted that similarity solutions are capable of providing a *local* description of some flow, their stability to non-self-similar perturbations is not addressed. Further, the existence or uniqueness of solutions to the similarity equations needs careful interpretation.

The problem to be addressed here is the flow between two *finite* disks, one rotating at constant angular speed Ω and the other at rest. The disks are separated a distance H apart. The horizontal extent of our problem remains to be addressed. In theoretical treatments of this problem, it has been customary to consider disks of infinite extent,[3,4] employing a similarity treatment. More recently, the question of existence and uniqueness of solutions in the similarity formulation has been raised.[5,6] The question as to the behavior of the flow between the two disks and in particular near the stationary disk as the speed of the rotating disk approaches infinity has not been satisfactorily addressed in this formulation and a long running difference of opinion concerning the nature of the flow between the two disks at *finite* radii continues. On the one hand, Batchelor[3] argues that boundary layers form on both disks, with the interior fluid rotating, whereas Stewartson[4] argues that a boundary layer forms only on the rotating disk, with the interior being essentially stationary. The difference of opinions may in part be related to the fact that the similarity formulation does not address the question of where the vortex lines terminate. All the vortex lines in this problem emanate from the rotating disk, and cannot terminate on the stationary disk nor in the fluid interior. Here, we do not attempt to address the issue of where the vortex lines in a radially unbounded flow between disks of infinite radius terminate. Instead, we consider the question of whether the similarity solutions are locally useful in describing the flow between *finite* disks. Self-similar treatments of this problem[7,8] are also inconclusive as they do not address where the vortex lines terminate. Some progress can be made by enclosing the disks, of finite radius R, by a cylindrical shroud also of radius R, as suggested by Rott and Lewellen.[1] The two simplest situations are for the cylindrical shroud, or sidewall, to either remain stationary or to co-rotate with the rotating disk. The two cases result in very different flows, and this can be traced to the difference in where the vortex lines terminate. In the stationary sidewall case, they terminate at the singularity where the edge of the rotating disk meets the stationary sidewall, whereas for the co-rotating sidewall case, they terminate at the singularity where the edge of the stationary disk meets the sidewall.

Of particular interest in these flows is how the boundary layers of the two disks couple with the interior flow. In these finite systems governed by the axisymmetric Navier–Stokes equations, do stable steady solutions exist that can at least locally be described by the similarity solutions? Further, is

there ''detailed matching'' between the vertical outflow from the stationary disk boundary layer and the vertical inflow into the rotating disk boundary layer, i.e., does the axial velocity out of one boundary layer match the axial velocity into the other boundary layer at every radial location?

For certain initial conditions, the two cases locally behave, at least for early times, as described by the semi-infinite flows corresponding to von Kármán[9] and Bödewadt.[10] In particular, for the stationary sidewall with the flow initially at rest, the flow near the rotating disk behaves very much like von Kármán's flow. However, in this finite shrouded case, there is no detailed matching between the two disk boundary layers, and the interior flow adjustment required to match the flow into and out of the disk boundary layers typically results in a flow far from geostrophic balance. In fact, recirculation zones develop on the axis and unsteady flow is also observed. This case has been studied extensively,[11–14] and will not be discussed further here.

When the initial condition is a rotating cylinder with the fluid in solid body rotation and the top endwall is impulsively stopped, the flow in the neighborhood of the top stationary disk is of Bödewadt form. Moore,[15] Schwiderski and Lugt,[16] Greenspan,[17] amongst others, suggest that the similarity solution of Bödewadt will not be realized as they expect the boundary layer to separate from the disk at some distance from the origin. However, this conjecture is questioned by Rott and Lewellen[18,1] who look at the shrouded flow with a stationary top and rotating side and bottom. They treat the disk boundary layers in a self-similar fashion and seek detailed matching between the vertical velocities entering and leaving the disk boundary layers. In this way, they derive an approximate equation for the angular momentum, $\Gamma = rv$, where v is the azimuthal component of velocity, halfway between the two disks. Their expression for Γ compares very well [Fig. 3 (Ref. 18) and Fig. 7 (Ref. 1)] with the experimental measurements of Maxworthy,[19] for $Re = \Omega R^2/\nu \approx 2\times 10^4$, where ν is the kinematic viscosity of the fluid. This then suggests that a self-similar treatment of both boundary layers, at least at steady state, is appropriate. However, the questions concerning the Bödewadt solution are still not addressed.

Bodonyi and Stewartson[20] and Stewartson, Simpson, and Bodonyi[21] look at the unsteady development of the Bödewadt layer in finite and infinite disks with solid body rotation far from the disks and conclude that the Bödewadt similarity solution exists. However, no stability analysis to non-self-similar perturbations (e.g., r-dependent perturbations) are considered.

Savaş,[22,23] in an attempt to investigate the stability of the Bödewadt solution, conducted experiments where the fluid inside a circular cylinder was initially in solid body rotation. Following an impulsive stop of the cylinder, the flow in the interior remains in solid body rotation for some time and the flow near the endwalls behaves locally like that corresponding to Bödewadt flow. He observed that for $Re > 2.5\times 10^3$ axisymmetric waves develop in the endwall boundary layers and propagate radially inwards, thus destroying their self-similar nature.

Lopez and Weidman[24] further investigated the impulsive spin-down in a cylinder in order to better understand the structure of the endwall boundary layers, in particular, the nature and origin of the circular waves. They determined that they are a mode of instability of the Bödewadt type flow near the stationary endwall, as suggested by Savaş.[23] By also conducting numerical experiments where only the endwalls were impulsively stopped while the sidewall continued to rotate, the effects of the centrifugal instability of the sidewall layer were isolated. They showed that the onset of circular endwall waves was not influenced by the presence of the sidewall, but is a local response to the structure of the boundary layers. However, due to the confined nature of the flow, the secondary meridional circulation tends to advect the vortex lines out towards the sidewall, and so the rotation of the interior could not be maintained.

Here, a further modification to the spin-down flow is considered. The modification is designed to keep the interior vortex lines, in the long time limit, as close as possible to a configuration corresponding to solid body rotation. This is done by maintaining the constant rotation of both the sidewall and the bottom endwall, following an impulsive stopping of the top endwall. In this way, the vortex lines emanate from the rotating endwall and are anchored to it for all time. Of course, the Ekman-like boundary layer flow on the rotating endwall sweeps the vortex lines radially outwards, but they remain anchored to the rotating disk, unlike the case considered by Lopez and Weidman[24] where the vortex lines were anchored to the corners between the stationary endwalls and the rotating sidewall. The resultant flow in the present investigation is much closer to the idealized flow of Bödewadt in the semi-infinite domain, and may be as close as possible to it in a physically realizable finite domain.

Pao[25] has also studied this flow using the axisymmetric Navier–Stokes equations. However, for $Re \geqslant 1000$ he was only able to follow the evolution from an initial state of solid body rotation for about three or four radians of time following the impulsive stop, and hence missed the development of the circular waves in the stationary endwall boundary layer and the characteristics of the flow at steady state.

In the following section, Sec. II, the governing equations and the numerical technique for their solution are outlined. The results for a shrouded pair of disks where their separation is equal to their radius are presented in Sec. III. The results cover a large dynamical range, from $Re = 0$ (Stokes flow) to $Re = 10^5$. For this range of Re, starting from a state of solid body rotation, and impulsively stopping the top endwall, our time-dependent computations evolve to a steady state, and the steady states for $Re > 10^3$ have many of the features of suggested by the similarity solutions. The transients however do not, and for $Re > 10^3$, the stationary endwall boundary layer supports inward propagating circular waves. For $Re \sim O(10^5)$, these circular waves become very nonlinear, and lead to vortical eruptions out of the boundary layer region deep into the interior.

II. GOVERNING EQUATIONS

The equations governing the flow are the axisymmetric Navier–Stokes equations, together with the continuity equation and appropriate boundary and initial conditions. It is

convenient to write these using a cylindrical polar coordinate system (r,ϑ,z), relative to a stationary observer with the origin at the center of the bottom disk and the positive z axial direction being towards the top disk. For axisymmetric flow, there exists a Stokes streamfunction ψ and the velocity vector in cylindrical polars is

$$\boldsymbol{u}=(u,v,w)=\left(-\frac{1}{r}\psi_z,\frac{1}{r}\Gamma,\frac{1}{r}\psi_r\right). \tag{1}$$

Subscripts denote partial differentiation with respect to the subscript variable. This form of the velocity automatically satisfies the continuity equation. It is also convenient to introduce a new variable, the angular momentum $\Gamma=rv$. Γ is proportional to the circulation and plays the role of a streamfunction for the meridional vorticity field.[26] In other words, contours of Γ in a meridional plane are cross-sections of vortex surfaces (vortex lines), just as contours of ψ are cross-sections of streamsurfaces (streamlines). These give the local direction of the vorticity and velocity vectors in the plane, respectively, and the azimuthal components of the vectors give the degree to which the vectors are directed out of the plane. The vorticity field corresponding to (1) is

$$\boldsymbol{\omega}=(\xi,\eta,\zeta)=\left(-\frac{1}{r}\Gamma_z,-\frac{1}{r}\nabla_*^2\psi,\frac{1}{r}\Gamma_r\right),$$

where

$$\nabla_*^2=()_{zz}+()_{rr}-\frac{1}{r}()_r.$$

The axisymmetric Navier–Stokes equations, in terms of ψ, Γ, and η, are

$$D\Gamma=\frac{1}{Re}\nabla_*^2\Gamma, \tag{2}$$

and

$$D(\eta/r)=\frac{1}{Re}\left\{\nabla^2(\eta/r)+\frac{2}{r}(\eta/r)_r\right\}+(\Gamma^2/r^4)_z, \tag{3}$$

where

$$\nabla_*^2\psi=-r\eta, \tag{4}$$

$$D=()_t-\frac{1}{r}\psi_z()_r+\frac{1}{r}\psi_r()_z,$$

$$\nabla^2=()_{zz}+()_{rr}+\frac{1}{r}()_r,$$

and $Re=\Omega R^2/\nu$. The length scale is the radius of the cylinder R and the time scale is $1/\Omega$. The other governing non-dimensional parameter is the cylinder aspect ratio H/R, H being the cylinder height.

The boundary conditions are:

(1) on the axis, $r=0$, we have $\psi=0$, $\eta=0$, and $\Gamma=0$;
(2) on the rotating sidewall, $r=1$, we have $\psi=0$, $\eta=-\psi_{rr}$, and $\Gamma=1$;
(3) on the stationary top endwall, $z=1$, we have $\psi=0$, $\eta=-\psi_{zz}/r$, and $\Gamma=0$;
(4) on the rotating bottom endwall, $z=0$, we have $\psi=0$, $\eta=-\psi_{zz}/r$, and $\Gamma=r^2$.

A. Computational technique

The governing equations are discretized using second-order centered differences to approximate all spatial derivatives. A non-uniform grid is used to resolve the thin endwall boundary layers. The grid is stretched in the axial direction by

$$z_j=[z_j'-b\sin(2\pi z_j')]H/R,$$

where $z_j'=(j-1)/(nz-1)$ for $j=1\rightarrow nz$, and employs uniform spacing in the radial direction. All the results presented have $b=0.1$.

Time integration employs an explicit second-order predictor-corrector scheme. The elliptic equation (4) is solved using generalized cyclic reduction, and second-order one-sided differences are used to discretize the derivative boundary conditions.

Further details of the computational technique are given in Lopez and Weidman.[24]

III. RESULTS

In this section, we show a continuous branch of steady solutions from $Re=0$ to $Re=10^5$. This does not imply, by any means, the uniqueness of these solutions. However, they are stable to time-dependent axisymmetric perturbations. Some preliminary experiments at $Re\approx1.1\times10^4$, conducted by Kittleman and Weidman using Hart's facility, were reported earlier,[27] and show that the waves in the stationary endwall layer remain axisymmetric. Snap-shots of the development of the flow in the stationary endwall boundary layer are presented in Fig. 1. The experiment consisted of a circular cylinder of radius 23.2 cm and height 19.3 cm, completely filled with water, and Kalliroscope flakes were used for visualizing the flow. The water temperature was ≈24 °C. Initially, the fluid was in solid body rotation with the cylinder, then at $t=0$, the top endwall (made of Plexiglas) was stopped. The snap-shots correspond to non-dimensional times $2.0\leqslant t\leqslant12.0$, where the time scale used is the rotation rate of the cylinder $\Omega=0.226$ rad s^{-1}. The experiment was conducted to see if the flow produced the axisymmetric waves in the neighborhood of parameter space of interest, and the results are included here to qualitatively show this to be the case.

More detailed experiments and three-dimensional computations are planned to further investigate the stability of these solutions to non-axisymmetric perturbations, especially for larger Re.

A. The steady solutions

We begin by examining the solutions once a steady state has been reached. In the following subsection, the transients associated with the higher ($>10^3$) Re cases will be discussed.

The Stokes problem ($Re=0$) can be solved analytically. Pao[25] and Khalili and Rath[28] provide the unique solution for

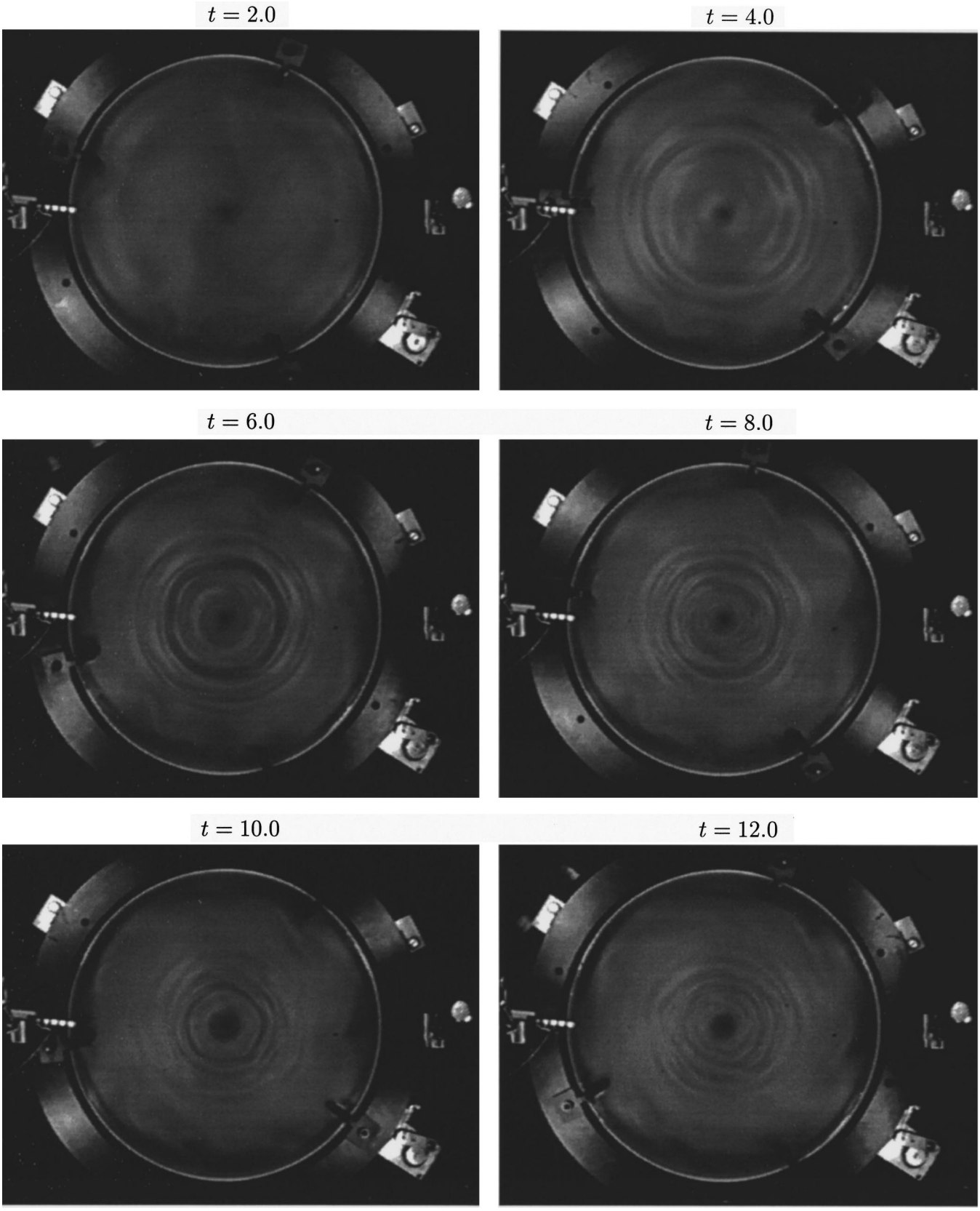

FIG. 1. Snap-shots at non-dimensional times as indicated, following the impulsive stop at $t=0$, of the development of the boundary layer on the stationary disk. The flow corresponds to $Re=1.1\times10^4$ and $H/R=0.83$.

this case (Khalili and Rath[28] also provide analytic solutions when each endwall and the sidewall rotate at different constant speeds) in terms of an infinite series of Bessel and trigonometric functions. Figure 12 in Pao[25] is a contour plot of Γ (the vortex lines) in a meridional plane. Here $(Re=0)$, the concept of a boundary layer does not make sense, but we see that we have a non-trivial flow that approaches solid body rotation as the distance from the station-

ary disk is increased. This is a finite radius disk version of the Bödewadt flow situation.

For non-zero Re, we solve the governing equations numerically. In all cases, we solve the initial value problem with solid body rotation as the initial condition, and the top endwall is impulsively stopped at $t=0$. The computed solution for Γ at $Re=1$ is virtually indistinguishable from the $Re=0$ solution presented in Pao.[25] The form of the singularity at the junction between the rotating sidewall and the stationary endwall is independent of Re. In comparing our computations with the analytic solution, we see that the computations have no difficulty in resolving this singularity. Figure 2 gives the numerical solutions, at steady state, for a range of Re as indicated. The spatial and temporal resolutions used in each case are given in Table I. These indicate that for $Re<10$, the flow is in the Stokes flow limit, where Γ is independent of Re, η, and ψ; and η and ψ scale with Re.

For $Re\geqslant 10^3$, the computed flows at steady state show distinct features of boundary layers on both the stationary and rotating disks. The boundary layer on the stationary disk has the characteristic spatial oscillations associated with the Bödewadt solution, and that on the rotating disk is characteristic of the extension of the von Kármán solution to the case when the outer flow is rotating at a slower rate.[29] Note the spatial oscillations in the vortex lines (Γ) near the rotating disk.

For $Re\geqslant 10^3$ and $r<0.5$, the flow is virtually independent of z outside of the boundary layers and has $\eta\approx 0$. (Note that the contours are non-uniformly spaced, with more contour intervals concentrated near zero, as detailed in the figure captions.) These features indicate that these flows, at steady state, should be well described by the similarity solutions (cf. Rogers and Lance[7]).

Rott and Lewellen[1] consider the question of detailed matching for the flow between a stationary and a rotating disk enclosed by a co-rotating sidewall. Using a simple implementation of the momentum-integral method, they derived an expression for the angular momentum (Γ) distribution of the interior flow which will permit a detailed matching between the two disk boundary layers, which they assumed to be laminar. The computed solutions shown in Fig. 2 suggest that these assumptions are reasonable. Their expression for Γ is

$$\Gamma=\frac{0.55\Omega r^2}{0.55+1.26(1-(r/R)^{4/3})^{3/4}}.$$

Figure 3 shows their Γ/r^2 estimate, along with the computed Γ/r^2 at the midplane for $Re=10^3$, 10^4, and 10^5. Rott and Lewellen[1] compared their expression for Γ/r^2 with the experimental measurements of Maxworthy,[19] corresponding to $Re\approx 2\times 10^4$. The comparison between theory based on laminar detailed matching, experiment, and computations of the axisymmetric Navier–Stokes equations shows very good agreement. This suggests that the flow between a stationary and a rotating disk, shrouded by a co-rotating sidewall, can be described by a self-similar formulation at steady state.

In Fig. 4, axial variations of v and η at $r=0.5$ in the vicinity of each disk are plotted. The axial direction in each case is scaled by $Re^{1/2}$ (but we do not scale the values of v or η). This shows that the flow for $Re\geqslant 10^3$ is self-similar, i.e., the boundary layer thickness on each disk scales with $Re^{1/2}$.

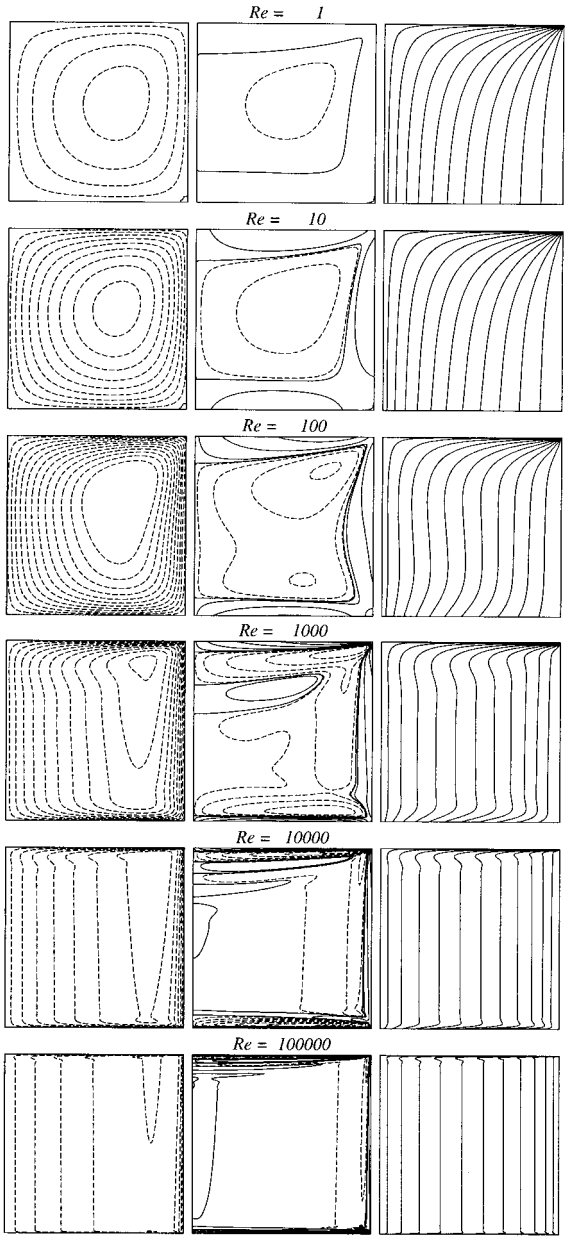

FIG. 2. Contours of ψ, η, and Γ, at steady state, for $H/R=1.0$ and Re as indicated. Table I gives the spatial and temporal resolutions used in each case. The contour levels are non-uniformly spaced, with 12 positive (solid lines) and 12 negative (dashed lines), determined by c_level $(i)=\max(variable)\times(i/12)^3$ and c_level$(i)=\min(variable)\times(i/12)^3$, respectively, with $i=1\rightarrow 12$. For all plots the following have been used: $\max(\psi)=0$, $\min(\psi)=-7.5\times 10^{-3}$, $\max(\eta)=100$, $\min(\eta)=-25$, $\max(\Gamma)=1$, and $\min(\Gamma)=0$.

This would all suggest that the story is over. However, all we have so far is that when the flow has reached steady state, then a self-similar treatment is valid and that there is detailed matching between the disk boundary layers, except in the neighborhood of the sidewall. In many cases however,

TABLE I. Spatial and temporal resolution used in the computations shown in Fig. 3.

Re	$nr\times nz$	δt
1	51×51	1.25×10^{-5}
10	51×51	1.25×10^{-4}
10^2	51×51	1.25×10^{-3}
10^3	101×101	5×10^{-3}
10^4	301×201	1×10^{-2}
10^5	601×401	5×10^{-3}

one is interested in the dynamics of the transient flow following the impulsive stopping of the top endwall, e.g., in turbomachinery applications. It would be useful to know if a self-similar treatment of the transient flow is also valid. This issue is addressed next.

B. Transients following the impulsive stop

The transient flow following the impulsive stopping of the top endwall is virtually indistinguishable, for early times ($t<10$), from that in the top half of a cylinder initially in solid body rotation following an impulsive stopping of both its endwalls. In turn, Lopez and Weidman[24] demonstrate that flow is indistinguishable from the impulsive stopping of the entire cylinder for early times, except in the immediate vicinity of the sidewall. In particular, in the present flow for $Re>10^3$, we observe the development of axisymmetric waves in the stationary disk boundary layer. Figure 5(a) shows the temporal development of these waves in the $Re=10^4$, $H/R=1$ case. The corresponding cases considered in Lopez and Weidman[24] have $H/R=2$, and their Fig. 3 gives the early time development of the waves. Comparing those with Fig. 5(a) one sees that the transient flow in all three cases, which for very early times corresponds to solid body rotation meeting a stationary endwall, does not remain self-similar, losing self-similarity to these axisymmetric waves.

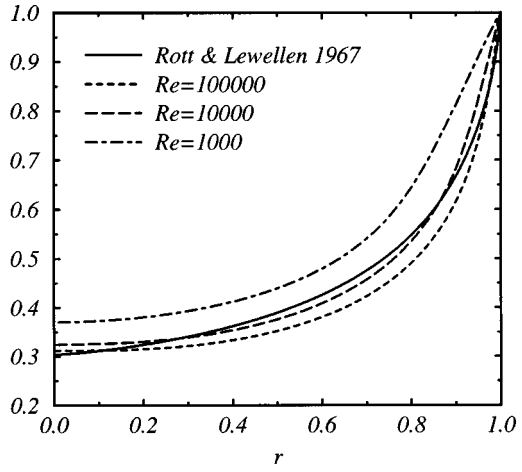

FIG. 3. Plot of the radial distribution of Γ/r^2 in the interior from Rott and Lewellen's[1] theory, and of Γ/r^2 at the cylinder half-height, $z=H/2R$, from the computations at Re as indicated.

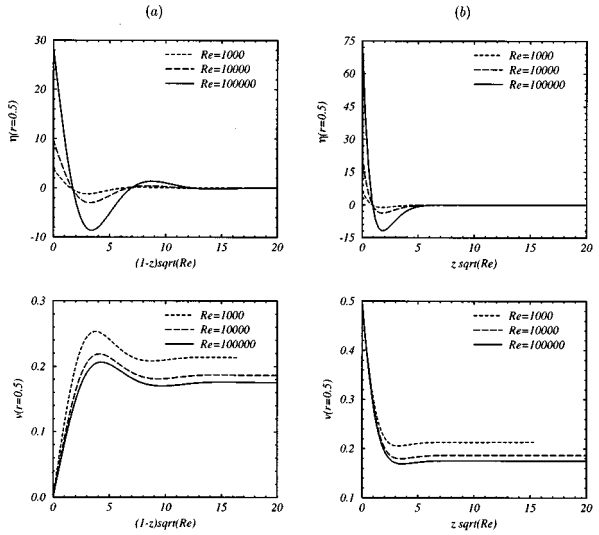

FIG. 4. Boundary layer profiles of η and v, at $r=0.5$, for various Re as indicated, corresponding to (a) the top stationary endwall, and (b) the bottom rotating endwall. The axial direction, z, for each case is scaled by $Re^{1/2}$.

For Re up to $O(10^4)$, we find that the axisymmetric waves are confined to the boundary layer region, that they travel radially inwards, and within a few rotation times ($t\sim15$), the boundary layer no longer supports them. The space-time diagrams in Fig. 6 give a good indication of the longevity of the waves, as well as their speed. The figure consists of contours of η on the top endwall (Bödewadt), the sidewall, and the bottom endwall (Ekman). The horizontal direction is time, from 0 to 60, and the vertical is space, starting from the axis on the bottom rotating endwall, going out to its edge then up the sidewall, and then in along the stationary endwall to the axis. For $Re=10^4$, the waves are present only in the boundary layer. They have maximum amplitude at about the axial location corresponding to the first inflection point in the axial variation of Γ (the vortex lines) and in the neighborhood of $r=0.5$. This is where the axial gradients in Γ are greatest, and hence where the turning of axial vorticity into the azimuthal direction via the $(\Gamma^2/r^4)_z$ term in (3) is greatest. At this Re there is no ''separation'' of the boundary layer and the waves decay smoothly as they approach the axis. The decay of the waves as $r\to0$ is possibly due to the axisymmetric constraint that the axis is both a streamline and a vortex line, thus the flow is ''straightened out'' as it approaches $r=0$. The result is that near $r=0$, there are no inflection points in Γ or ψ to support the waves (see Fig. 2). The deceleration of the waves as they approach $r=0$ is very distinct in the space–time plots (Fig. 6).

As Re is increased, the waves behave more nonlinearly. At $Re=2\times10^4$, the space–time plot (Fig. 6) shows evidence of successive waves pairing at $r\approx0.5$. This is most evident during the active times $5<t<10$, where the track of every second wave ''disappears'' following the merger with the preceding wave. The deceleration of the waves as they propagate inwards, together with the increased frequency (non-dimensional) with which they are produced at higher

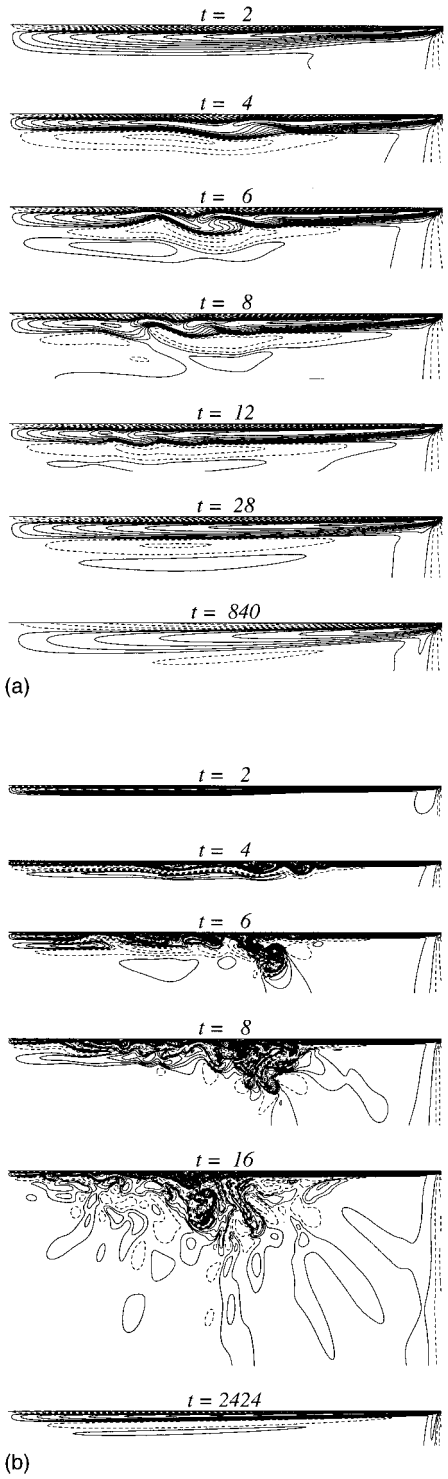

FIG. 5. Contours of η, in the vicinity of the stationary top endwall, $z=H/R$, at various times as indicated, for $H/R=1$ and (a) $Re=10^4$, (b) $Re=10^5$. The contour levels are non-uniformly spaced, with 20 positive (solid lines) and 20 negative (dashed lines), determined by $c\_\text{level}(i)=\max(\eta)\times(i/20)^2$ and $c\_\text{level}(i)=\min(\eta)\times(i/20)^2$, respectively, with $i=1\rightarrow 20$. For all plots, $\max(\eta)=150$ and $\min(\eta)=-50$.

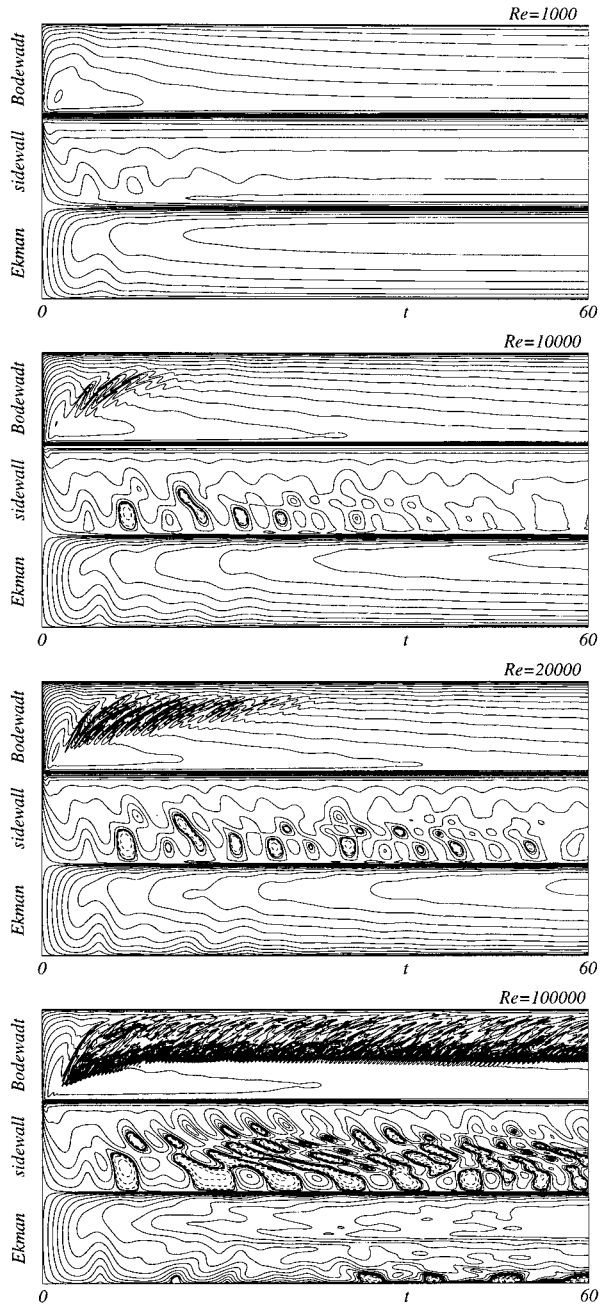

FIG. 6. Space–time plots for $H/R=1$ and Re as indicated, consisting of η contours on the bottom endwall (Ekman), sidewall, and the top endwall (Bödewadt). Time increases horizontally from $t=0$ to $t=60$. The contour levels are non-uniformly spaced, with 20 positive (solid lines) and 20 negative (dashed lines), determined by $c\_\text{level}(i)=\max(\eta)\times(i/20)^3$ and $c\_\text{level}(i)=\min(\eta)\times(i/20)^3$, respectively, with $i=1\rightarrow 20$. For all plots, $\max(\eta)=100$ and $\min(\eta)=-100$.

Re (see Fig. 6), are the primary reasons for the pairing of successive waves. The nonlinear behavior of the waves is much greater at $Re=10^5$. Here, not only is there merger between successive waves, but there are also ''back waves'' which travel radially outwards essentially on the second inflection point in the axial variation of Γ (of course, this is difficult to see as the vortex lines are greatly affected by these waves, however an animation of the solutions is indicative of this behavior). These back waves have azimuthal vorticity of the opposite sign to the first waves identified (corresponding to the change in sign of Γ_z), and at $Re=10^5$, Fig. 5(b) shows at $t=6$ the pairing up of a forward and a back wave to form a dipole like structure which erupts out of the

boundary layer. It is highly unlikely that these structure are stable to non-axisymmetric perturbations, but they are of interest as there are still unexplained occurrences of boundary layer eruptions in rotating flows.[30]

Schwiderski and Lugt[16] conjecture that the Bödewadt flows are unstable due to an inflection point instability. They find that inflection points in the velocity profiles are present for $\Omega(\alpha+1/\beta)^2/\nu \geqslant 9$, where α is the thickness of the boundary layer and $1/\beta$ is twice the radius of curvature of the boundary layer at the axis of rotation. The radius of curvature of the boundary layer can be determined from the zero contour of η in the boundary layer. The curvature is quite pronounced at low Re, is non-uniform with r, and decreases with Re, as indicated in Fig. 2. They[16] expect boundary layer separation to result. We have not made any serious attempt to convert their Reynolds number based on the characteristic thickness of the boundary layer to our Reynolds number based on the radius of the cylinder, however, it is reasonable that their value of 9 corresponds to our $Re \sim 10^3$, where inflection points just begin to be evident (e.g., Figs. 2 and 4). In contrast to their expectations, we do not find anything like boundary layer separations until Re is a couple of orders of magnitude larger than that at which inflection points first appear. Further, for $Re \sim 10^4$ the inflection point leads to waves (Fig. 5), but there is no boundary layer separation in the usual sense. In summary, we agree with Schwiderski and Lugt[16] that when an inflection point develops in the Bödewadt layer, it is unstable in that it loses its self-similar form due to the growth of axisymmetric waves, however their conjecture that this also leads to boundary layer separation is not supported by our computations. We also find that a re-adjustment of the flow through interactions between the primary and the secondary flow serves to damp out the waves and the final steady state, even for $Re = 10^5$, consists of a boundary layer with inflection points and is reasonably well described in self-similar terms. The non-linear interaction between the primary and the secondary flows leads to a re-distribution of the vortex lines away from solid body rotation to another rotating flow which is essentially independent of the axial direction in the interior and has a radial distribution close to that derived by Rott and Lewellen.[1] For larger Re it takes a very long time $[t \sim O(10^3)]$ to reach this steady state and the flow is very sensitive to small changes. In the following subsection we consider the sensitivity of the steady solutions to small changes in rotation rates.

C. Transients following low Rossby number changes

The steady flow is more sensitive at higher Re, as would be expected. However, here we shall illustrate the sensitivity of a moderate $Re = 10^4$ solution to small changes in the rotation rate of the lower disk and sidewall, i.e., small changes in Re. These changes are measured in terms of a Rossby number Ro, where

$$Ro = (\Omega_{\text{final}} - \Omega_{\text{initial}})/\Omega_{\text{final}}, \quad \text{for } \Omega_{\text{final}} > \Omega_{\text{initial}},$$

and

$$Ro = (\Omega_{\text{final}} - \Omega_{\text{initial}})/\Omega_{\text{initial}}, \quad \text{for } \Omega_{\text{final}} < \Omega_{\text{initial}}.$$

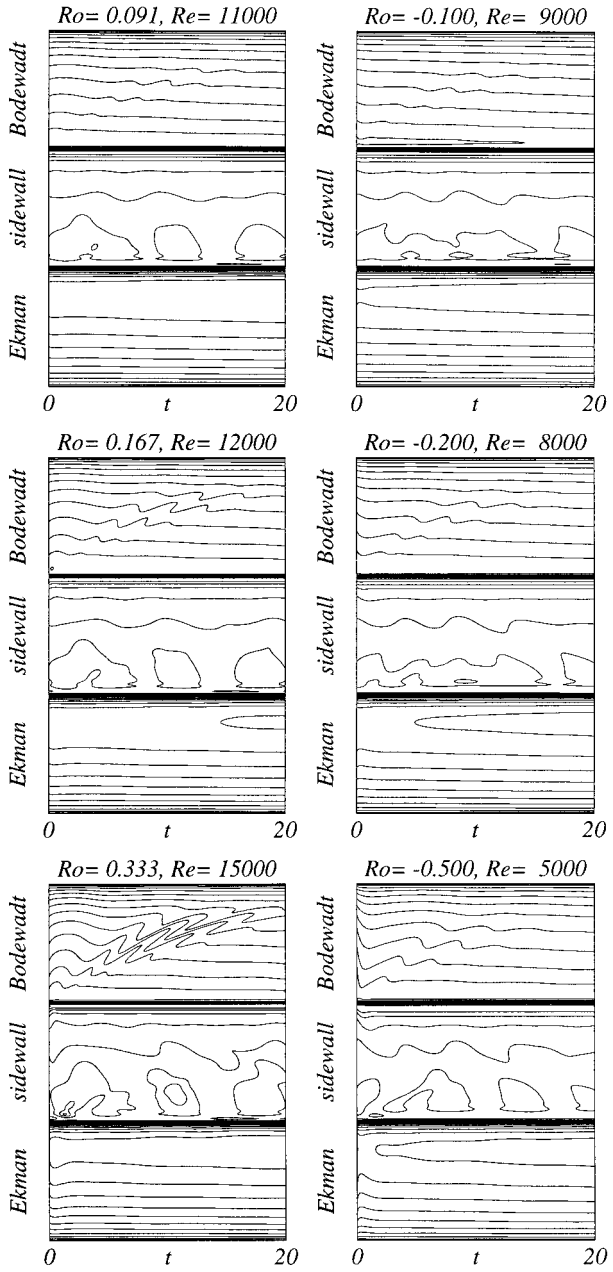

FIG. 7. Space–time plots as in Fig. 6, with $H/R = 1$. The initial condition at $t = 0$, corresponds to the $Re = 10^4$ steady state solution, with the rotation of the bottom and sidewall impulsively changes by an amount measured by Ro (the corresponding final Re is indicated also). The contour levels are non-uniformly spaced, with 20 positive (solid lines) and 20 negative (dashed lines), determined by $c\_\text{level}(i) = \max(\eta) \times (i/20)^3$ and $c\_\text{level}(i) = \min(\eta) \times (i/20)^3$, respectively, with $i = 1 \rightarrow 20$. For all plots, $\max(\eta) = 100$ and $\min(\eta) = -100$.

Figure 7 gives space–time plots of η for a range of Ro. Even for quite small Ro, both for a spin-up and a spin-down of the $Re = 10^4$ solution, there is clear evidence of the formation of the axisymmetric waves and a transient violation of the self-similar form of the flow. Note that spin-up is relatively more sensitive than spin-down. At larger Re this sensitivity is expected to be even greater.

IV. CONCLUSIONS

The Bödewadt type flow in a finite rotating cylinder, where solid body rotation meets a stationary endwall following an impulsive stop of the endwall, is unstable to axisymmetric waves once Re is large enough for inflection points in the vortex lines (Γ) to develop in the axial direction. However, in the long time limit this confined flow does not have $\Gamma \propto r^2$ in the interior. The resultant radial distribution of Γ essentially allows for detailed matching between the boundary layers (except in the immediate vicinity of the sidewall) and leads to boundary layer structures that are essentially self-similar. Neither the rotating nor the stationary endwall layers correspond directly to von Kármán's or Bödewadt's solutions, but they are of these types. The flow in the interior is neither solid body rotation (as needed for Bödewadt flow) or rest (as needed for von Kármán flow), but instead is given by Γ as shown in Fig. 3. Both boundary layers have inflection points, the one corresponding to the stationary endwall having much larger axial gradients in Γ, and so is more susceptible to waves travelling radially along the inflection points following the slightest change (increase or decrease) in the rotation rate of the bottom and sidewall. At very large Re, we expect that even small changes in Ω will result in eruptions out of the stationary endwall boundary layers.

ACKNOWLEDGMENTS

The author is grateful for helpful discussions with Dick Bodonyi, Mike Foster, John Hart, and Patrick Weidman. Special thanks go to John Hart for kindly making his experimental apparatus available and to Scott Kittleman and Patrick Weidman for re-machining the stationary top endwall and performing the experiment. This work was partially funded by the National Science Foundation under Grant No. DMS-9512483.

[1]N. Rott and W. S. Lewellen, ''Boundary layers and their interactions in rotating flows,'' Prog. Aeronaut. Sci. **7**, 111 (1967).
[2]L. Durlofsky and J. F. Brady, ''The spatial stability of a class of similarity solutions,'' Phys. Fluids **27**, 1068 (1983).
[3]G. K. Batchelor, ''Note on a class of solutions of the Navier–Stokes equations representing steady rotationally-symmetric flow,'' Q. J. Mech. Appl. Math. **4**, 29 (1951).
[4]K. Stewartson, ''On the flow between two rotating coaxial disks,'' Proc. Cambridge Philos. Soc. **49**, 333 (1953).
[5]G. L. Mellor, P. J. Chapple, and V. K. Stokes, ''On the flow between a rotating and a stationary disk,'' J. Fluid Mech. **31**, 95 (1968).
[6]S. V. Parter, ''On the swirling flow between rotating coaxial disks: A survey,'' *Theory and Applications of Singular Perturbations*, edited by A. Dold and B. Ekmann, Lecture Notes in Mathematics, 1982, Vol. 942, p. 258.
[7]M. H. Rogers and G. N. Lance, ''The boundary layer on a disc of finite radius in a rotating fluid,'' Q. J. Mech. Appl. Math. **17**, 319 (1964).
[8]N. D. Nguyen, J. P. Ribault, and P. Florent, ''Multiple solutions for flow between coaxial disks,'' J. Fluid Mech. **68**, 369 (1975).
[9]Th. von Kármán, ''Über laminare und turbulente Reibung,'' Z. Angew. Math. Mech. **1**, 233 (1921).
[10]U. T. Bödewadt, ''Die Drehstr'ómung über festem Grunde,'' Z. Angew. Math. Mech. **20**, 241 (1940).
[11]M. P. Escudier, ''Observations of the flow produced in a cylindrical container by a rotating endwall,'' Exp. Fluids **2**, 189 (1984).
[12]J. M. Lopez, ''Axisymmetric vortex breakdown. Part 1. Confined swirling flow,'' J. Fluid Mech. **221**, 533 (1990).
[13]G. L. Brown and J. M. Lopez, ''Axisymmetric vortex breakdown. Part 2. Physical mechanisms,'' J. Fluid Mech. **221**, 553 (1990).
[14]J. M. Lopez and A. D. Perry, ''Axisymmetric vortex breakdown. Part 3. Onset of periodic flow and chaotic advection,'' J. Fluid Mech. **234**, 449 (1992).
[15]F. K. Moore, ''Three-dimensional boundary layer theory,'' Adv. Appl. Mech. **4**, 159 (1956).
[16]E. W. Schwiderski and H. J. Lugt, ''Rotating flows of von Kármán and B'Ödewadt,'' Phys. Fluids **7**, 867 (1964).
[17]H. P. Greenspan, *The Theory of Rotating Fluids* (Cambridge University Press, Cambridge, 1968).
[18]N. Rott and W. S. Lewellen, ''Examples of boundary layers in rotating flows,'' Agardograph **97**, 613 (1965).
[19]T. Maxworthy, ''The flow between a rotating disk and a co-axial, stationary disk,'' Space Programs Summary 37-27, Vol. 4, Sec. 327; Jet Propulsion Laboratory, Pasadena, CA, 1964.
[20]R. J. Bodonyi and K. Stewartson, ''Boundary-layer similarity near the edge of a rotating disk,'' J. Appl. Mech. **42**, 584 (1975).
[21]K. Stewartson, C. J. Simpson, and R. J. Bodonyi, ''The unsteady boundary layer on a rotating disk in a counter-rotating fluid. Part 2,'' J. Fluid Mech. **121**, 507 (1982).
[22]Ö. Savaş, ''Circular waves on a stationary disk in rotating flow,'' Phys. Fluids **26**, 3445 (1983).
[23]Ö. Savaş, ''Stability of Bödewadt flow,'' J. Fluid Mech. **183**, 77 (1987).
[24]J. M. Lopez and P. D. Weidman, ''Stability of stationary endwall boundary layers during spin-down,'' J. Fluid Mech. (accepted).
[25]H. -P. Pao, ''A numerical computation of a confined rotating flow,'' J. Appl. Mech. **37**, 480 (1970).
[26]S. L. Bragg and W. R. Hawthorne, ''Some exact solutions of the flow through annular cascade actuator discs,'' J. Aeronaut. Sci. **17**, 243 (1950).
[27]J. M. Lopez, ''Couplings between endwall boundary layers and rotating flows,'' Bull. Am. Phys. Soc. **40**, 2011 (1995).
[28]A. Khalili and H. J. Rath, ''Analytical solution for a steady flow of enclosed rotating disks,'' Z. Angew. Math. Phys. **45**, 670 (1994).
[29]F. Schultz-Grunow, ''Der Reibungswiderstand rotierender Scheiben in Geh'áusen,'' Z. Angew. Math. Mech. **15**, 191 (1935).
[30]M. L. Rozenzweig, D. H. Ross, and W. S. Lewellen, ''On secondary flows in jet-driven vortex tubes,'' J. Aerosp. Sci. **29**, 1142 (1962).